

# Synaptic Metaplasticity in Binarized Neural Networks

Axel Laborieux<sup>1,\*</sup>, Maxence Ernout<sup>1</sup>, Tifenn Hirtzlin<sup>1</sup>, and Damien Querlioz<sup>1,\*</sup>

<sup>1</sup>Université Paris-Saclay, CNRS, Centre de Nanosciences et de Nanotechnologies, 91120, Palaiseau, France.

\*axel.laborieux@c2n.upsaclay.fr, damien.querlioz@c2n.upsaclay.fr

## ABSTRACT

While deep neural networks have surpassed human performance in multiple situations, they are prone to catastrophic forgetting: upon training a new task, they rapidly forget previously learned ones. Neuroscience studies, based on idealized tasks, suggest that in the brain, synapses overcome this issue by adjusting their plasticity depending on their past history. However, such “metaplastic” behaviour has never been leveraged to mitigate catastrophic forgetting in deep neural networks. In this work, we highlight a connection between metaplasticity models and the training process of binarized neural networks, a low-precision version of deep neural networks. Building on this idea, we propose and demonstrate experimentally, in situations of multitask and stream learning, a training technique that prevents catastrophic forgetting without needing previously presented data, nor formal boundaries between datasets. We support our approach with a theoretical analysis on a tractable task. This work bridges computational neuroscience and deep learning, and presents significant assets for future embedded and neuromorphic systems.

## Introduction

In recent years, deep neural networks have experienced incredible developments, outperforming the state-of-the-art, and sometimes human performance, for tasks ranging from image classification to natural language processing<sup>1</sup>. Nonetheless, these models suffer from catastrophic forgetting<sup>2,3</sup> when learning new tasks: synaptic weights optimized during former tasks are not protected against further weight updates and are overwritten, causing the accuracy of the neural network on these former tasks to plummet<sup>4,5</sup> (see Fig. 1(a)). Balancing between learning new tasks and remembering old ones is sometimes thought of as a trade-off between plasticity and rigidity: synaptic weights need to be modified in order to learn, but also to remain stable in order to remember. This issue is particularly critical in embedded environments, where data is processed in real-time without the possibility of storing past data. Given the rate of synaptic modifications, most artificial neural networks were found to have exponentially fast forgetting<sup>6</sup>. This contrasts strongly with the capability of the brain, whose forgetting process is typically described with a power law decay<sup>7</sup>, and which can naturally perform continuous learning.

The neuroscience literature provides insights about underlying mechanisms in the brain that enable task retention. In particular, it was suggested by Fusi et al.<sup>6,8</sup> that memory storage requires, within each synapse, hidden states with multiple degrees of plasticity. For a given synapse, the higher the value of this hidden state, the less likely this synapse is to change: it is said to be consolidated. These hidden variables could account for activity-dependent mechanisms regulated by intercellular signalling molecules occurring in real synapses<sup>9,10</sup>. The plasticity of the synapse itself being plastic, this behaviour is named “metaplasticity”. The metaplastic state of a synapse can be viewed as a criterion of importance with respect to the tasks that have been learned throughout and therefore constitutes one possible approach to overcome catastrophic forgetting.

Until now, the models of metaplasticity have been used for idealized situations in neuroscience studies. However, intriguingly, in the field of deep learning, binarized neural networks<sup>11</sup> (or the closely related XNOR-NETs<sup>12</sup>) have a remote connection with the concept of metaplasticity that has so far never been explored. Binarized neural networks are neural networks whose weights and activations are constrained to the values +1 and −1. These networks were developed for performing inference with low computational and memory cost<sup>13–15</sup>, and surprisingly, can achieve

excellent accuracy on multiple vision<sup>12,16</sup> and signal processing<sup>17</sup> tasks. The training procedure of binarized neural networks involves a real value associated to each synapse which accumulates the gradients of the loss computed with binary weights. This real value is said to be “hidden”, as during inference, we only use its sign to get the binary weight. In this work, we interpret the hidden weight in binarized neural networks as a metaplastic variable that can be leveraged to achieve multitask learning. Based on this insight, we develop a learning strategy using binarized neural networks to alleviate catastrophic forgetting with strong biological-type constraints: previously-presented data can not be stored, nor generated, and the loss function is not task-dependent with weight penalties.

An important benefit of our synapse-centric approach is that it does not require a formal separation between datasets, which also allows the possibility to learn a single task in a more continuous fashion. Traditionally, if new data appears, the network needs to relearn incorporating the new data into the old data: otherwise the network will just learn the new data and forget what it had already learned. Through the example of the progressive learning of datasets, we show that our metaplastic binarized neural network, by contrast, can continue to learn a task when new data becomes available, without seeing the previously presented data of the dataset. This feature makes our approach particularly attractive for embedded contexts. The spatially and temporally local nature of the consolidation mechanism makes it also highly attractive for hardware implementations, in particular using neuromorphic approaches.

Our approach takes a remarkably different direction than the considerable research in deep learning that is now addressing the question of catastrophic forgetting. Many proposals consist in keeping or retrieving information about the data or the model at previous tasks: using data generation<sup>18</sup>, the storing of exemplars<sup>19</sup>, or in preserving the initial model response in some components of the network<sup>20</sup>. These strategies do not seem connected to how the brain avoids catastrophic forgetting, need a very formal separation of the tasks, and are not very appropriate for embedded contexts. A solution to solve the trade-off between plasticity and rigidity more connected to ours is to protect synaptic weights from further changes according to their “importance” for the previous task. For example, elastic weight consolidation<sup>3</sup> uses the diagonal elements of the Fisher information matrix of the model distribution with respect to its parameters to identify synaptic weights qualifying as important for a given task. In another work<sup>21</sup>, the consolidation strategy consists in computing an importance factor based on path integral. Finally,<sup>22</sup> uses the sensitivity of the network with respect to small changes in synaptic weights. In all these techniques, the desired memory effect is enforced by changing the loss function and does not emerge from the synaptic behaviour itself. This aspect requires a very formal separation of the tasks, and makes these models still largely incompatible with the constraints of biology and embedded contexts. The highly non-local nature of the consolidation mechanism also makes it difficult to implement in neuromorphic-type hardware.

Specifically, the contributions of the present work are the following:

- We interpret the hidden real value associated to each weight (or hidden weight) in binarized neural networks as a metaplastic variable, we propose a new training algorithm for these networks adapted to learning different tasks sequentially (Alg. 1).
- We show that our algorithm allows a binarized neural network to learn permuted MNIST tasks sequentially with an accuracy equivalent to elastic weight consolidation, but without any change to the loss function or the explicit computation of a task-specific importance factor. More complex sequences such as MNIST - Fashion-MNIST can also be learned sequentially with test accuracy on both tasks having no degradation with respect to the accuracy reached on a single task.
- We show that our algorithm enables to learn the Fashion-MNIST and the CIFAR-10 datasets by learning sequentially each subset of these datasets, which we call the stream-type setting.
- We show that our approach has a mathematical justification in the case of a tractable quadratic binary task where the trajectory of hidden weights can be derived explicitly.

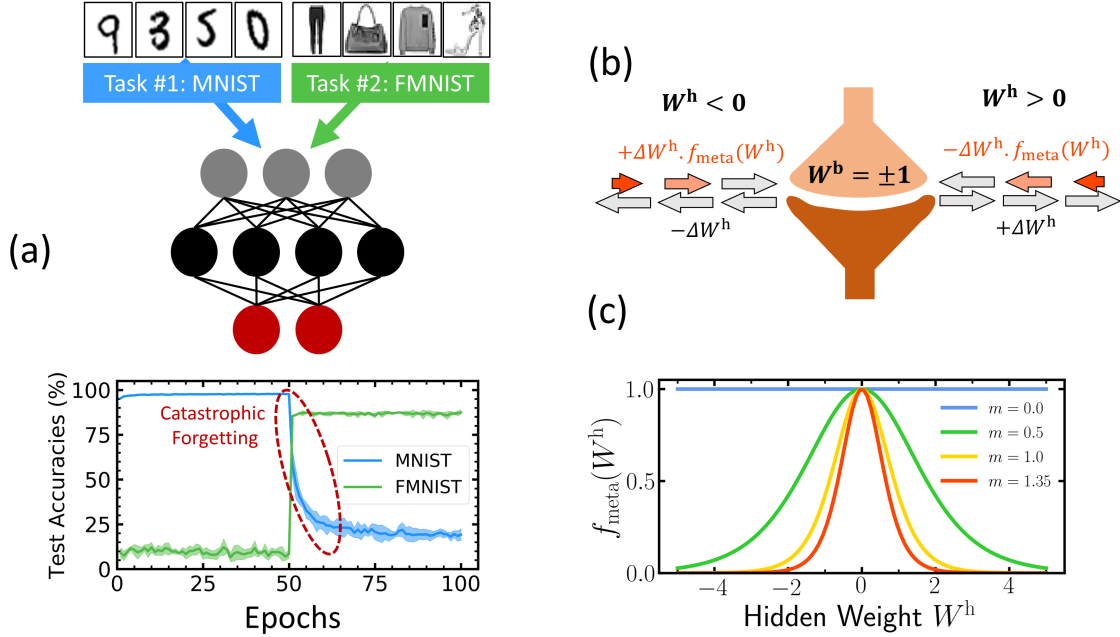


**Figure 1. Problem setting and illustration of our approach.** (a) Problem setting: two training sets (here MNIST and Fashion-MNIST) are presented sequentially to a fully connected neural network. When learning MNIST (epochs 0 to 50), the MNIST test accuracy reaches 97%, while the Fashion-MNIST accuracy stays around 10%. When learning Fashion-MNIST (epochs 50 to 100), the associated test accuracy reaches 85% while the MNIST test accuracy collapses to  $\sim 20\%$  in 25 epochs: this phenomenon is known as “catastrophic forgetting”. (b) Illustration of our approach: in a binarized neural network, each synapse incorporates a hidden weight  $W^h$  used for learning and a binary weight  $W^b = \text{sign}(W^h)$  used for inference. Our method, inspired by neuroscience works in the literature<sup>6</sup>, amounts to regarding hidden weights as metaplastic states that can encode memory across tasks and thereby alleviate forgetting. With regards to the conventional training technique of binarized neural network, it consists in modulating some hidden weight updates by a function  $f_{\text{meta}}(W^h)$  whose shape is indicated in (c). This modulation is applied to negative updates of positive hidden weights, and to positive updates of negative hidden weights.  $f_{\text{meta}}(|W^h|)$  being a decreasing function, this modulation makes the hidden weights signs less likely to switch back when they grow in absolute value.

## Multitask Learning with Metaplastic Binarized Neural Networks

The training process of conventional binarized neural networks relies on updating hidden real weights associated with each synapse, using loss gradients computed with binary weights. The binary weights are the signs of the hidden real weights, and are used in the equations of both the forward and backward passes. By contrast, the hidden weights are updated as a result of the learning rule, which therefore affects the binary weights only when the hidden weight changes sign - the detailed training algorithms are presented in Supplementary Algorithms 1 and 2 of Supplementary Note 1. Hidden weights magnitudes have no impact on inference: two given binary weights of a binarized neural network may be equal to one, but their corresponding hidden weight may differ depending on the history of the training process.

---

**Algorithm 1** Our modification of the BNN training procedure to implement metaplasticity.  $W^h$  are the hidden weights,  $\theta^{\text{BN}}$  are Batch Normalization parameters,  $U_W$  and  $U_\theta$  are the parameter updates prescribed by the Adam algorithm<sup>23</sup>,  $(x, y)$  is a batch of labelled training data,  $m$  is the metaplasticity parameter, and  $\eta$  is the learning rate. “ $\cdot$ ” denotes the element-wise product of two tensors with compatible shapes. The difference between our implementation and the non-metaplastic implementation (recovered for  $m = 0$ ) lies in the condition lines 6 to 9.  $f_{\text{meta}}$  is applied element-wise with respect to  $W^h$ . “cache” denotes all the intermediate layers computations needed to be stored for the backward pass. The details of the Forward and Backward functions are provided in Supplementary Note 1.

---

*Input:*  $W^h, \theta^{\text{BN}}, U_W, U_\theta, (x, y), m, \eta$ .

*Output:*  $W^h, \theta^{\text{BN}}, U_W, U_\theta$ .

```

1:  $W^b \leftarrow \text{Sign}(W^h)$                                 ▷ Computing binary weights
2:  $\hat{y}, \text{cache} \leftarrow \text{Forward}(x, W^b, \theta^{\text{BN}})$         ▷ Perform inference
3:  $C \leftarrow \text{Cost}(\hat{y}, y)$                                 ▷ Compute mean loss over the batch
4:  $(\partial_W C, \partial_\theta C) \leftarrow \text{Backward}(C, \hat{y}, W^b, \theta^{\text{BN}}, \text{cache})$     ▷ Cost gradients
5:  $(U_W, U_\theta) \leftarrow \text{Adam}(\partial_W C, \partial_\theta C, U_W, U_\theta)$ 
6: if  $U_W \cdot W^b > 0$  then                                ▷ If  $U_W$  prescribes to decrease  $|W^b|$ 
7:    $W^h \leftarrow W^h - \eta U_W \cdot f_{\text{meta}}(m, W^h)$         ▷ Metaplastic update
8: else
9:    $W^h \leftarrow W^h - \eta U_W$ 
10: end if
11:  $\theta^{\text{BN}} \leftarrow \theta^{\text{BN}} - \eta U_\theta$ 
12: return  $W^h, \theta^{\text{BN}}, U_W, U_\theta$ 

```

---

Described as such, the training process of binarized neural networks is intriguingly similar to the one of metaplastic Hopfield networks in<sup>6</sup>: it prescribes to binarize the weight for the computation of the preactivations or “synaptic currents”, and to update a metaplastic hidden variable for learning. This comparison suggests that the hidden weights in binarized neural networks could also be used as metaplastic variables. In our work, we show that we can use the hidden weights as a criterion for importance to learn several tasks sequentially with one binarized neural network, which involves one single set of synaptic weights. However, for this purpose, the training procedure of binarized neural networks needs to be adapted. Based on the work of Fusi<sup>6</sup>, our intuition is that binary weights with high hidden weight values are relevant to the current task and can be consolidated: the learning process should ensure that the greater the hidden real value, the more difficult to switch back. For lack of such a blocking mechanism, there cannot be a long term memory across tasks since the number of updates required to learn a given task is heuristically equal to the number of updates required to unlearn it. We therefore introduce the function  $f_{\text{meta}}$  to provide an asymmetry which differentiates between updates towards zero hidden weights and away from zero for equivalent gradient absolute values (see Fig. 1(b)). The higher the hidden weight, the more difficult it is for the binary weight to switch sign, which is very similar in spirit to the cascade of metaplastic states introduced in<sup>6</sup>. The strength of the metaplasticity effect is characterized by the real parameter  $m$  of function  $f_{\text{meta}}$  (see Fig. 1(c)), the case

$m = 0$  corresponding to the conventional binarized neural network case. The detailed training algorithm is provided in Algorithm 1, and its practical implementation is described in Methods.

We first test the validity of our approach by learning sequentially multiple versions of the MNIST dataset where the pixels have been permuted, which constitutes a canonical benchmark for continual learning<sup>2</sup>. We train a binarized neural network with two hidden layers of 4,096 units using Algorithm 1 with several metaplasticity  $m$  values and 40 epochs per task (see Methods). Fig. 2 shows this process of learning six tasks. The conventional binarized neural network ( $m = 0.0$ ) is subject to catastrophic forgetting: after learning a given task, the test accuracy quickly drops upon learning a new task. Increasing the parameter  $m$  gradually prevents the test accuracy on previous tasks from decreasing with eventually the  $m = 1.35$  binarized neural network (Fig. 2(d)) managing to learn all six tasks with test accuracies comparable with the 97.4% test accuracy achieved by the BNN trained on one task only (see Table. 1).

Figs. 2(g) and 2(h) show the distribution of the metaplastic hidden weights after learning Task 1 and Task 2 in the second layer. The consolidated weights of the first task in Fig. 2(g) correspond to hidden weights between zero and five in magnitude. We observe in Fig. 2(g) that around  $10^7$  of binary weights still have hidden weights near zero after learning one task. These weights correspond to synapses that repeatedly switched between  $+1$  and  $-1$  binary weights during the training of the first task, and thus of little importance for the first task. These synapses were therefore not consolidated, and are then available for learning another task, as shown in Fig. 2(h). After learning the second task (Fig. 2(h)), we can distinguish between hidden weights of synapses consolidated for Task 1 and for Task 2.

	No consolidation ( $m = 0.0$ )	Random Consolidation	Elastic Weight Consolidation	<b>Metaplasticity (<math>m = 1.35</math>)</b>
Task 1	$9.2 \pm 2.2$	$29.0 \pm 2.9$	$96.8 \pm 0.7$	<b><math>96.9 \pm 0.6</math></b>
Task 2	$7.8 \pm 1.3$	$29.0 \pm 4.2$	$97.2 \pm 0.2$	<b><math>97.2 \pm 0.3</math></b>
Task 3	$9.3 \pm 2.0$	$32.7 \pm 4.7$	$96.9 \pm 0.2$	<b><math>96.9 \pm 0.2</math></b>
Task 4	$9.0 \pm 1.7$	$35.1 \pm 4.1$	$96.6 \pm 0.2$	<b><math>96.4 \pm 0.4</math></b>
Task 5	$13.2 \pm 3.7$	$47.7 \pm 8.8$	$96.8 \pm 0.3$	<b><math>96.7 \pm 0.8</math></b>
Task 6	$97.4 \pm 0.2$	$96.8 \pm 0.2$	$96.8 \pm 0.3$	<b><math>97.3 \pm 0.1</math></b>

**Table 1.** Binarized neural network test accuracies on six permuted MNISTs at the end of training for different settings. We indicate mean and standard deviation over five trials, for a conventional (non-metaplastic) BNN ( $m = 0.0$ ), consolidation of synapses with random importance factors, elastic weight consolidation (EWC)<sup>3</sup> computed with parameter  $\lambda_{\text{EWC}} = 5 \cdot 10^3$ , and our metaplastic binarized neural network approach with parameter  $m = 1.35$ .

Table 1 presents a comparison of the results obtained using our technique with a random consolidation of weights, and with elastic weight consolidation<sup>3</sup>, implemented on the same binarized neural network architecture (see Methods). We see that the random consolidation approach does not allow multitask learning. On the other hand, our approach achieves a performance similar to elastic weight consolidation for learning six permuted MNISTs with the given architecture, although unlike elastic weight consolidation the consolidation is based on an entirely local rule without changing the loss function.

Supplementary Figure 1 shows a more detailed analysis of the performance of our approach when learning up to ten MNIST permutations, and for varying sizes of the binarized neural network, highlighting the connection between network size and its capacity in terms of number of tasks.

As a control experiment, we also applied Algorithm 1 to a full precision network, except for the weight binarization step described in line one. Fig. 2(e) and Fig. 2(f) show the final accuracy of each task at the end of learning for a binarized neural network and a real valued weights deep neural network respectively, with the same architecture. The full precision network final test accuracy of each task for the same range of  $m$  values cannot

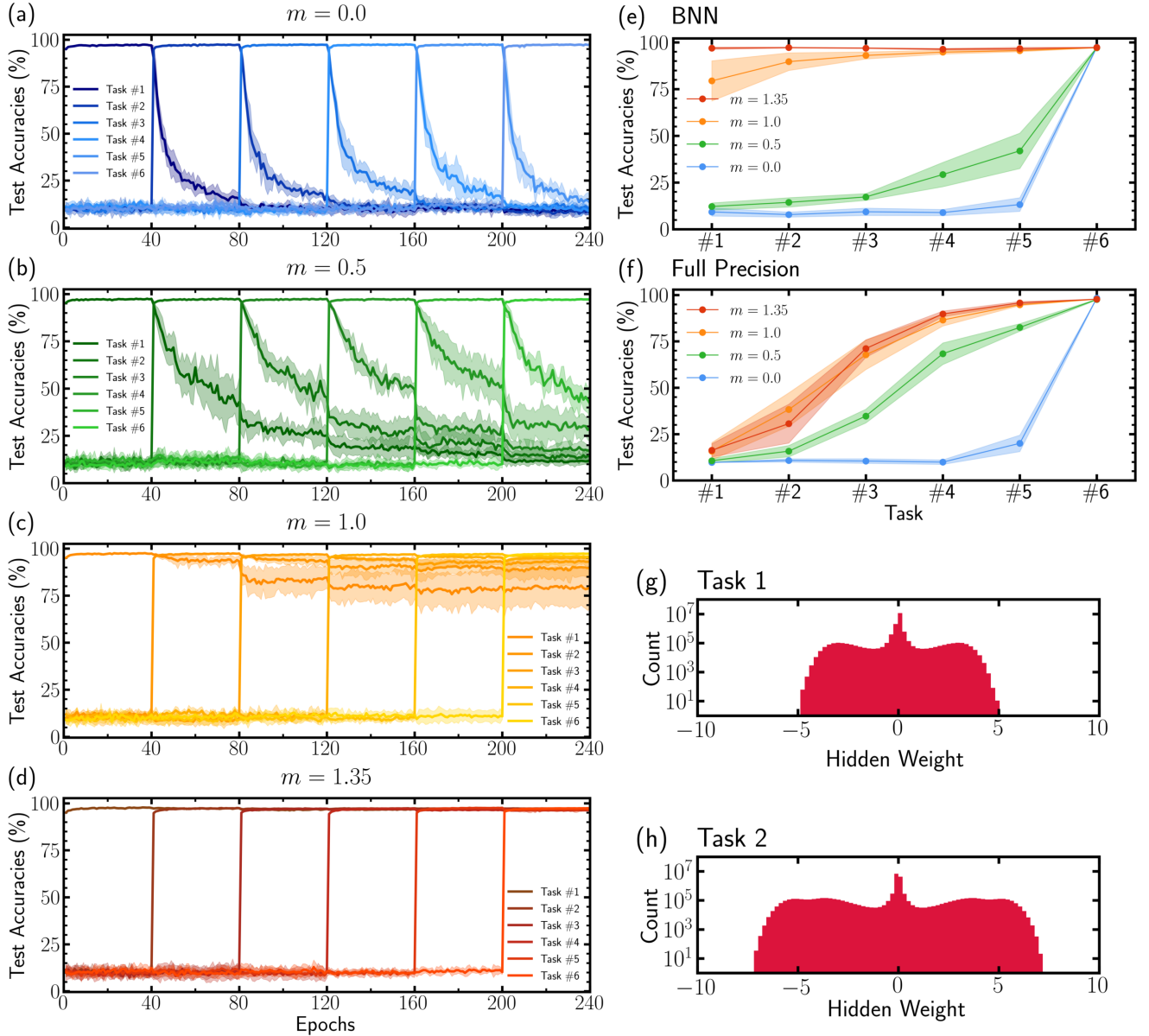


**Figure 2. Permuted MNIST learning task.** Binarized neural network learning six tasks sequentially for several values of the metaplastic parameter  $m$ . (a)  $m = 0$  corresponds to a conventional binarized neural network (b)  $m = 0.5$  (c)  $m = 1.0$  (d)  $m = 1.35$ . Curves are averaged over five runs and shadows correspond to one standard deviation. (e,f) Final test accuracy on each task after the last task has been learned. The dots indicate the mean values over five runs, and the shaded zone one standard deviation. (e) corresponds to a binarized neural network and (f) corresponds to our method applied to a real valued weights deep neural network with the same architecture. (g,h) Hidden weights distribution of a  $m = 1.35$ , two hidden layers of 4,096 units binarized neural network after learning for 40 epochs each task (g) one permuted MNIST and (h) two permuted MNISTs.



retain more than three tasks with accuracy above 90%. This highlights that our weight consolidation strategy is tied specifically to the use of a binarized neural network.

This experimental result points out the fundamentally different meaning of hidden weights in a binarized neural network and of real weights in a full precision neural network respectively. In full precision networks, the inference is carried out using the real weights, in particular the loss function is also computed using these weights. Conversely in binarized neural networks, the inference is done with the binary weights and the loss function is also evaluated with these binary weights, which has two major consequences. First, the hidden weights do not undergo the same updates as the weights of a full precision network. Second, a synapse whose hidden weight is positive and which is prescribed a positive update consequently will not affect the loss, nor its gradient at the next learning iteration since it only takes into account the sign of the hidden weights. Hidden weights in binarized neural networks consequently have a natural tendency to spread over time (Fig. 2(g,h)) they are not technically weights, but a trace of the history of the network updates that is relevant for memory effects.

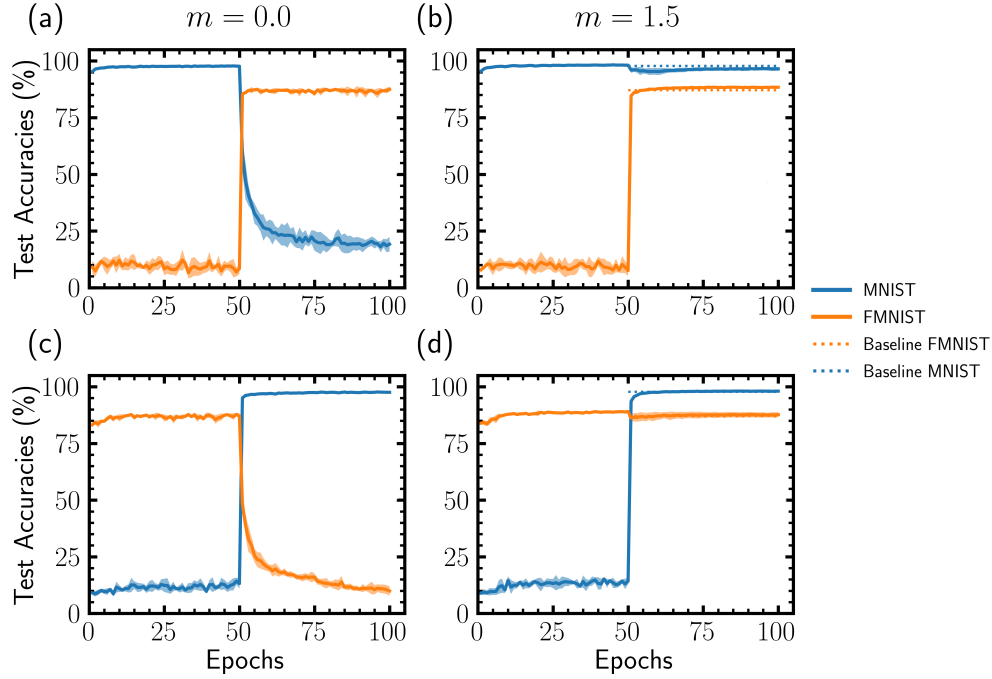


**Figure 3. MNIST/Fashion-MNIST sequential learning.** Binarized neural network learning MNIST and Fashion-MNIST sequentially ((a) and (b)) or Fashion-MNIST and MNIST ((c) and (d)) for two values of the metaplastic parameter  $m$ .  $m = 0$  corresponds to a conventional BNN ((a) and (c)),  $m = 1.5$  is a metaplastic BNN ((b) and (d)). Curves are averaged over five runs and shadows correspond to one standard deviation.

To test further the ability of our binarized neural network to learn several tasks sequentially, we sequentially train a binarized neural network on two tasks in a more difficult situation. When learning permuted versions of MNIST, the relevant input features do not overlap extensively between tasks which makes it easier for the network to learn sequentially. For this reason, we now train a binarized neural network with two hidden layers of 4,096 units to learn sequentially the MNIST dataset and the Fashion-MNIST dataset<sup>24</sup> which consists of fashion items images belonging to ten classes. Fig. 3(b) shows the result of the training of a  $m = 1.5$  binarized neural network, with 50 epochs on MNIST and 50 epochs on Fashion-MNIST (Fig. 3(d) shows the reverse training order). Figs. 3(a) and (c) also show the result for the conventional binarized neural network ( $m = 0$ ). Baselines define the accuracies the binarized neural network would have obtained had it been trained on each of these tasks separately. In the context of Fig. 3, we consider the baseline of Fashion-MNIST is realized in Fig. 3(a) (orange curve after 100 epochs) and the baseline of MNIST in Fig. 3(c) (blue curve after 100 epochs). We observe that the metaplastic binarized neural network is able

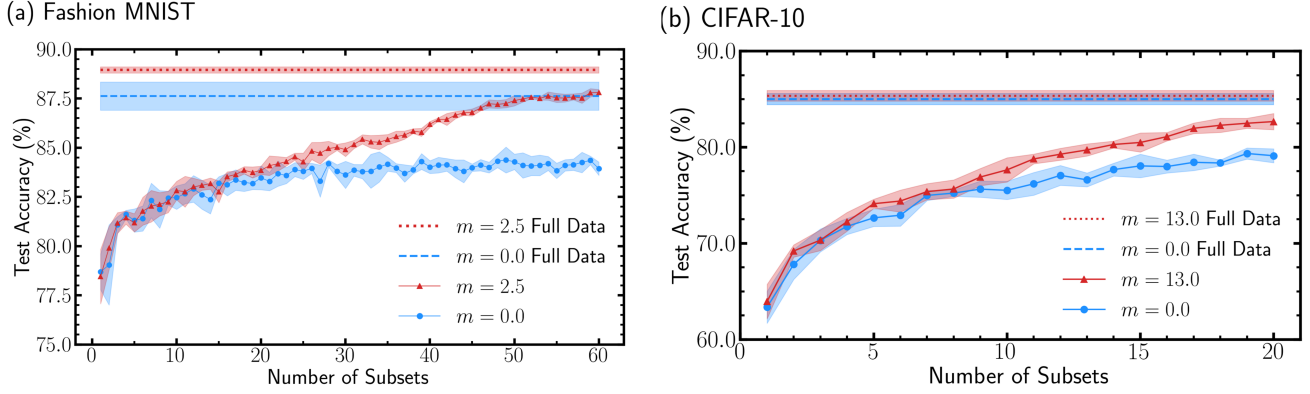


**Figure 4. Stream learning experiments.** (a) Progressive learning of the Fashion-MNIST dataset. The dataset is split into 60 parts consisting of only 1,000 examples, and containing all ten classes. Each sub dataset is learned for 20 epochs. The dashed lines represent the accuracies reached when the training is done on the full dataset for 20 epochs so that all curves are obtained with the same number of optimization steps. (b) Progressive learning of the CIFAR-10 dataset. The dataset is split into 20 parts, consisting of only 2,500 examples. Each sub dataset is learned for 200 epochs. The dashed lines represent the accuracies reached when the training is done on the full dataset for 200 epochs. Shadows correspond to one standard deviation around the mean over five runs.

to learn both tasks sequentially with baseline accuracies regardless of the order chosen to learn the tasks.

### Stream Learning: Learning one Task from Subsets of Data

We have shown that the hidden weights of binarized neural networks can readily be used as importance factors for synaptic consolidation. Therefore, in our approach, it is not required to compute an explicit importance factor for each synaptic weight. Our consolidation strategy is carried out simultaneously with the weight update, and locally in space as consolidation only involves the hidden weights. The absence of formal dataset boundaries in our approach is important to tackle another aspect of catastrophic forgetting where all the training data of a given task is not available at the same time. In this section, we use our method to address this situation, which we call “stream learning”: the network learns one task but can only access one subset of the full dataset at a given time. Subsets of the full dataset are learned sequentially and the data of previous subsets cannot be accessed in the future.

We first consider the Fashion-MNIST dataset, split into 60 subsets presented sequentially during training (see Methods). The learning curves for regular and metaplastic binarized neural networks are shown in Fig. 4(a), the dashed lines corresponding to the accuracy reached by the same architecture trained on the full dataset after full convergence. We observe that the metaplastic binarized neural network trained sequentially on subsets of data performs as well as the non-metaplastic binarized neural network trained on the full dataset. The difference in accuracy between the baselines can be explained by our consolidation strategy gradually reducing the number of weights able to switch, therefore acting as a learning rate decay (the mean accuracy achieved by a binarized neural network with  $m = 0$  trained with a learning rate decay on all the data is 88.8%, equivalent to the metaplastic baseline in Fig. 4(a)).

In order to see if the advantage provided by metaplastic synapses holds for convolutional networks and harder tasks, we then consider the CIFAR-10 dataset, with a binarized version of a Visual Geometry Group (VGG) convolutional neural network (see Methods). CIFAR-10 is split into 20 sub datasets of 2,500 examples. The test accuracy curve of the metaplastic binarized neural network exhibits a gap with baseline accuracies smaller than the non-metaplastic one. Our metaplastic binarized neural network can thus gain new knowledge from new data without forgetting previously learned unavailable data.

Because our consolidation strategy does not involve changing the loss function and the batch normalization



settings are common across all subsets of data, the metaplastic binarized neural network gains new knowledge with each subset of data without any information about subsets boundaries. This feature is especially useful for embedded applications, and is not currently possible in alternative approaches of the literature to address catastrophic forgetting.

## Mathematical Interpretation

We now provide a mathematical interpretation for the hidden weights of binarized neural networks: we show in archetypal situations that the larger a hidden weight gets while learning a given task, the bigger the loss increase upon flipping the sign of the associated binary weight, and consequently the more important they are with respect to this task. For this purpose, we define a quadratic binary task, an analytically tractable and convex counterpart of a binarized neural network optimization task. This task, defined formally in Supplementary Note 3, consists in finding the global optimum on a landscape featuring a uniform (Hessian) curvature. The gradient used for the optimization is evaluated using only the sign of the parameters  $W^h$  (Fig. 5(a)), in the same way that binarized neural networks employ only the sign of hidden weights for computing gradients during training. In Supplementary Note 3, we demonstrate theoretically that throughout optimization on the quadratic binary task, if the uniform norm of the weight optimum vector is greater than one, the hidden weights vector diverges. Fig. 5(a) shows an example in two dimensions where such a divergence is seen. This situation is reminiscent of the training of binarized neural networks on practical tasks, where the divergence of some hidden weights is observed. In the particular case of a diagonal Hessian curvature, a correspondence exists between diverging hidden weights and components of the weight optimum greater than one in absolute value. We can derive an explicit form for the asymptotic evolution of the diverging hidden weights while optimizing: the hidden weights diverge linearly:  $W_{i,t}^h \sim \tilde{W}_i^h t$  with a speed proportional to the curvature and the absolute magnitude of the global optimum (see Supplementary Note 3). Given this result, we can prove the following theorem (see Supplementary Note 3):

**Theorem 1.** *Let  $W$  optimize the quadratic binary task with optimum weight  $W^*$  and curvature matrix  $H$ , using the optimization scheme:  $W_{t+1}^h = W_t^h - \eta H \cdot (\text{sign}(W_t^h) - W^*)$ . We assume  $H$  equal to  $\text{diag}(\lambda_1, \dots, \lambda_d)$  with  $\lambda_i > 0$ ,  $\forall i \in \llbracket 1, d \rrbracket$ . Then, if  $|W_i^*| > 1$ , the variation of loss resulting from flipping the sign of  $W_{i,t}^h$  is:*

$$\Delta_i \mathcal{L}(W_t) \sim 2\lambda_i + 2 \frac{|\tilde{W}_i^h|}{\eta} \quad \text{as } t \rightarrow +\infty \quad (1)$$

This theorem states that the increase in the loss induced by flipping the sign of a diverging hidden weight is asymptotically proportional to the sum of the curvature and a term proportional to the hidden weight. Hence the correlation between high valued hidden weights and important binary weights.

Interestingly, this interpretation, established rigorously in the case of a diagonal Hessian curvature, may generalize to non-diagonal Hessian cases. Fig. 5 for example illustrates the correspondence between hidden weights and high impact on the loss by sign change on a quadratic binary task (Fig. 5(b)) with a 500-dimensional non-diagonal Hessian matrix (see Methods for the generation procedure). Fig. 5(c,d,e) finally shows that this correspondence extends to a practical binarized neural network situation, trained on MNIST. In this case, the cost variation  $\mathbb{E}_{\text{data}}(\Delta \mathcal{L})$  upon switching binary weights signs increases monotonically with the magnitudes of the hidden weights (see Methods for implementation details). These results provide an interpretation as to why hidden weights can be thought of as local importance factors useful for continual learning applications.

## Discussion and Related Works

Addressing catastrophic forgetting with ideas from both neuroscience and machine learning has led us to find an artificial neural network with richer synapses behaviours that can perform continual learning without requiring an overhead computation of task-related importance factors. The continual learning capability of metaplastic binarized neural networks emerges from its intrinsic design, which is in stark contrast with other consolidation strategies<sup>3,21,22</sup>. The resulting model is more autonomous because the optimized loss function is the same across all tasks. Metaplastic

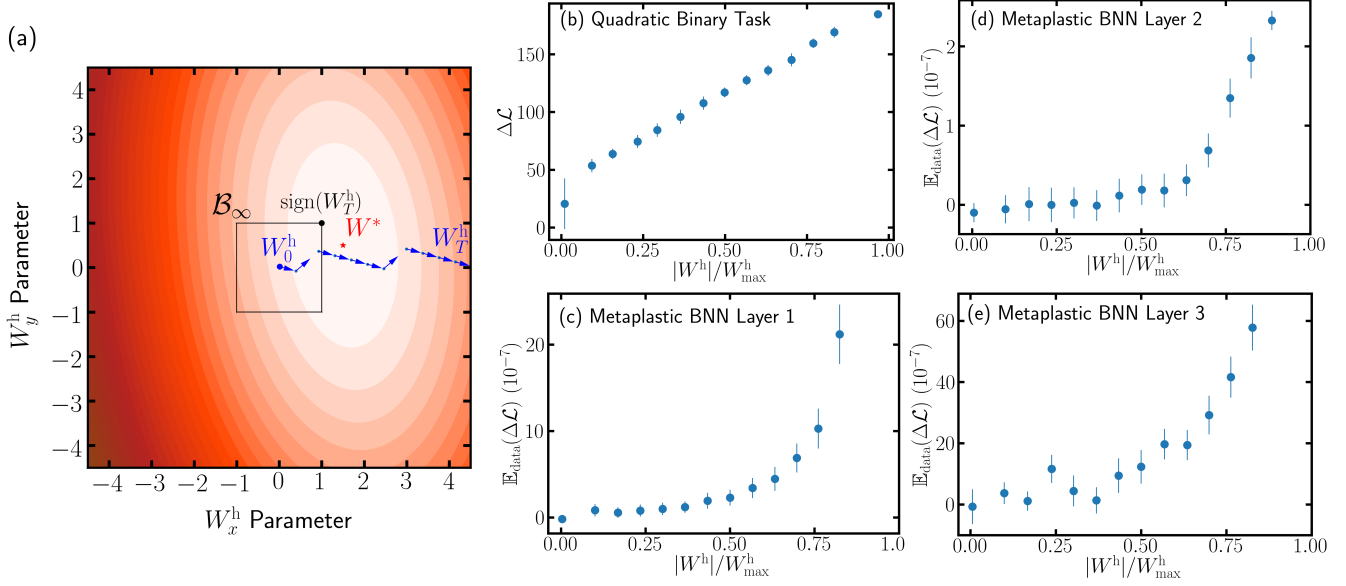


**Figure 5. Interpretation of the meaning of hidden weights.** (a) Example of hidden weights trajectory in a two-dimensional quadratic binary task. One hidden weight  $W_x^h$  diverges because the optimal hidden weight vector  $W^*$  has uniform norm greater than one (Lemma 2 of Supplementary Note 3). (b) Mean increase in the loss occurred by switching the sign of a hidden weight as a function of the normalized value of the hidden weight, for a 500-dimensional quadratic binary task. The mean is taken by assigning hidden weights to bins of increasing absolute value. The leftmost point corresponds to hidden weights staying bounded. (c,d,e) Increase in the loss occurred by switching the sign of hidden weights as a function of the normalized absolute value of the hidden weight in a binarized neural network trained on MNIST. The scales differ because the layers have different numbers of weights and thus different relative importance. See Methods for implementation details.

synapses enable binarized neural networks to learn several tasks sequentially similarly to related works, but more importantly, our approach takes the first steps beyond a more fundamental limitation of deep learning, namely the need for a full dataset to learn a given task. A single autonomous model able to learn a task from small amounts of data while still gaining knowledge, approaching to some extent the way the brain acquires new information, paves the way for widespread use of embedded hardware for which it is impossible to store large datasets.

Additionally, taking inspiration from the metaplastic behaviour of actual synapses of the brain resulted in a strategy where the consolidation is local in space and time. This makes this approach particularly suited for artificial intelligence dedicated hardware and neuromorphic computing approaches, which can save considerable energy by employing circuit architectures optimized for the topology of neural network models, and therefore limiting data movements<sup>25</sup>. The fact that our approach builds on synapses with rich behaviour also resonates with the progress of nanotechnologies, which can provide compact and energy-efficient electronic devices able to mimic neuroscience-inspired models<sup>26–29</sup>. This also evidences the benefit of taking inspiration from biology with regards to purely mathematically-motivated approaches: they tend to be naturally compatible with the constraints of hardware developments and can be amenable for the development of energy-efficient artificial intelligence.

In conclusion, we have shown that the hidden weights involved in the training of binarized neural networks are excellent candidates as metaplastic variables that can be efficiently leveraged for continual learning. We have implemented long term memory into binarized neural networks by modifying the hidden weight update of synapses. Our work highlights that binarized neural networks might be more than a low precision version of deep neural networks, as well as the potential benefits of the synergy between neurosciences and machine learning research, which for instance aims to convey long term memory to artificial neural networks. We have also mathematically

justified our technique in a tractable quadratic binary problem. Our method allows for online synaptic consolidation directly from model behaviour, which is important for neuromorphic dedicated hardware, and is also useful for a variety of settings subject to catastrophic forgetting.

## Acknowledgements

This work was supported by European Research Council Starting Grant NANOINFER (reference: 715872). The authors would like to thank L. Herrera-Diez, J. Thiele, G. Hocquet, P. Bessière, T. Dalgaty and J. Grolier for discussion and invaluable feedback on the manuscript.

## Author Contributions

AL developed the Pytorch code used in this project and performed all subsequent simulations. AL and ME carried the mathematical analysis of the Mathematical Interpretation section. TH provided the initial idea for the project, and an initial Numpy version of the code. Authors ME and TH contributed equally to the project. DQ directed the work. All authors participated in data analysis, discussed the results and co-edited the manuscript.

## Conflict of Interest Statement

The authors declare that they have no known competing financial interests or personal relationships that could have appeared to influence the work reported in this paper.

## Methods

### Metaplasticity-Inspired Training of Binarized Neural Networks

The binarized neural networks studied in this work are designed and trained following the principles introduced in<sup>11</sup> - specific implementation details are provided in Supplementary Note 2. These networks consist of binarized layers where both weight values and neuron activations assume binary values meaning  $\{+1, -1\}$ . Binarized neural networks can achieve high accuracy on vision tasks<sup>12, 16</sup>, provided that the number of neurons is increased with regards to real neural networks. Binarized neural networks are especially promising for AI hardware because unlike conventional deep networks which rely on costly matrix-vector multiplications, these operations for binarized neural networks can be done in hardware with XNOR logic gates and pop-count operations, reducing the power consumption by several orders of magnitude<sup>15</sup>.

In this work, we propose an adaptation of the conventional binarized neural network training technique to provide binarized neural networks with metaplastic synapses. We introduce the function  $f_{\text{meta}} : \mathbb{R}^+ \times \mathbb{R} \rightarrow \mathbb{R}$  to provide an asymmetry, at equivalent gradient value and for a given weight, between updates towards zero hidden value and away from zero. Alg. 1 describes our optimization update rule and the unmodified version of the update rule is recovered when  $m = 0.0$  due to condition (2) satisfied by  $f_{\text{meta}}$ .  $f_{\text{meta}}$  is defined such that:

$$\forall x \in \mathbb{R}, f_{\text{meta}}(0, x) = 1, \quad (2)$$

$$\forall m \in \mathbb{R}^+, f_{\text{meta}}(m, 0) = 1, \quad (3)$$

$$\forall m \in \mathbb{R}^+, \partial_x f_{\text{meta}}(m, 0) = 0, \quad (4)$$

$$\forall m \in \mathbb{R}^+, \lim_{|x| \rightarrow +\infty} f_{\text{meta}}(m, x) = 0. \quad (5)$$

Conditions (3) and (4) ensure that near-zero real values, the weights are free to switch in order to learn. Condition (5) ensures that the farther from zero a real value is, the more difficult it is to make the corresponding weight switch back. In all the experiments of this paper, we use :

$$f_{\text{meta}}(m, x) = 1 - \tanh^2(m \cdot x). \quad (6)$$

The parameter  $m$  controls how fast binary weights are consolidated (Fig. 1(c)). The specific choice of  $f_{\text{meta}}$  is made to have a variety of plasticity over large ranges of time steps (iteration steps) with an exponential dependence as in<sup>6</sup>. Specific values of the hyperparameters can be found in Supplementary Note 2.

### Multitask training experiments

A permuted version of the MNIST dataset consists of a fixed spatial permutation of pixels applied to each example of the dataset. We also train a full precision (32-bits floating point) version of our network with the same architecture for comparison, but with tanh activation function instead of sign. The learned parameters in batch normalization are not binary and therefore cannot be consolidated by our metaplastic strategy. Therefore, in our experiments, the binarized and full precision neural networks have task-specific batch normalization parameters in order to isolate the effect of weight consolidation on previous tasks test accuracies.

The elastic weight consolidation control is trained with parameter  $\lambda_{\text{EWC}} = 5 \cdot 10^3$ . The random consolidation presented in Tab. 1 consists in computing the same importance factors as elastic weight consolidation but then randomly shuffling the importance factors of the synapses.

### Stream learning experiments

For Fashion-MNIST experiments, we use a metaplastic binarized neural network of two 1,024 units hidden layers. The dataset is split into 60 subsets of 1,000 examples each, and each subset is learned for 20 epochs. (All classes are represented in each subset.)

For CIFAR-10 experiments, we use a binary version of VGG-7 similarly to<sup>11</sup>, with six convolution layers of 128-128-256-256-512-512 filters and kernel sizes of 3. Dropout with probability 0.5 is used in the last two fully connected layers of 2,048 units. Data augmentation is used within each subset with random crop and random rotation.

### Sign Switch in a binarized neural network

Two major differences between the quadratic binary task and the binarized neural network are the dependence on the training data and the relative contribution of each parameter which is lower in the case of the BNN than in the quadratic binary task. The procedure for generating Fig. 5(c,d,e) has to be adapted accordingly. Bins of increasing normalised hidden weights are created, but instead of computing the cost variation for a single sign switch, a fixed amount of weights are switched within each bin so as to increase the contribution of the sign switch on the cost variation. The resulting cost variation is then normalised with respect to the number of switched weights. An average is done over several realizations of the hidden weights to be switched. Given the different sizes of the three layers, the amounts of switched weights per bins for each layer are respectively 1,000, 2,000, and 100.

### Positive Symmetric Definite Matrix Generation

To generate random positive symmetric definite matrices we first generate the diagonal matrix of eigenvalues  $D = \text{diag}(\lambda_1, \dots, \lambda_d)$  with a uniform or normal distribution of mean  $\mu$  and variance  $\sigma$  and ensure that all eigen values are positive. We then use the subgroup algorithm described in<sup>30</sup> to generate a random rotation  $R$  in dimension  $d$ . We then compute  $H = R^T \cdot D \cdot R$ .

### Data and Code Availability

Throughout this work, all simulations are performed using Pytorch 1.1.0. The source codes used in this work are freely available online in the Github repository:

<https://github.com/Laborieux-Axel/SynapticMetaplasticityBNN>,

All used datasets (MNIST, Fashion-MNIST, CIFAR-10) are available in the public domain.

### References

1. LeCun, Y., Bengio, Y. & Hinton, G. Deep learning. *Nature* **521**, 436–444 (2015).

2. Goodfellow, I. J., Mirza, M., Xiao, D., Courville, A. & Bengio, Y. An empirical investigation of catastrophic forgetting in gradient-based neural networks. In *Proceedings of International Conference on Learning Representations (ICLR)* (2014).
3. Kirkpatrick, J., Pascanu, R., Rabinowitz, N., Veness, J., Desjardins, G., Rusu, A. A., Milan, K., Quan, J., Ramalho, T., Grabska-Barwinska, A. *et al.* Overcoming catastrophic forgetting in neural networks. *Proc. national academy sciences* **114**, 3521–3526 (2017).
4. French, R. M. Catastrophic forgetting in connectionist networks. *Trends cognitive sciences* **3**, 128–135 (1999).
5. McClelland, J. L., McNaughton, B. L. & O'Reilly, R. C. Why there are complementary learning systems in the hippocampus and neocortex: insights from the successes and failures of connectionist models of learning and memory. *Psychol. review* **102**, 419 (1995).
6. Fusi, S., Drew, P. J. & Abbott, L. F. Cascade models of synaptically stored memories. *Neuron* (2005).
7. Wixted, J. T. & Ebbesen, E. B. On the form of forgetting. *Psychol. science* **2**, 409–415 (1991).
8. Benna, M. K. & Fusi, S. Computational principles of synaptic memory consolidation. *Nat. neuroscience* **19**, 1697 (2016).
9. Abraham, W. C. & Bear, M. F. Metaplasticity: the plasticity of synaptic plasticity. *Trends neurosciences* **19**, 126–130 (1996).
10. Abraham, W. C. Metaplasticity: tuning synapses and networks for plasticity. *Nat. Rev. Neurosci.* **9**, 387–387 (2008).
11. Courbariaux, M., Hubara, I., Soudry, D., El-Yaniv, R. & Bengio, Y. Binarized neural networks: Training deep neural networks with weights and activations constrained to +1 or -1. *arXiv preprint arXiv:1602.02830* (2016).
12. Rastegari, M., Ordonez, V., Redmon, J. & Farhadi, A. Xnor-net: Imagenet classification using binary convolutional neural networks. In *European Conference on Computer Vision*, 525–542 (Springer, 2016).
13. Conti, F., Schiavone, P. D. & Benini, L. Xnor neural engine: A hardware accelerator ip for 21.6-fj/op binary neural network inference. *IEEE Transactions on Comput. Des. Integr. Circuits Syst.* **37**, 2940–2951 (2018).
14. Bankman, D., Yang, L., Moons, B., Verhelst, M. & Murmann, B. An always-on 3.8μj/86% cifar-10 mixed-signal binary cnn processor with all memory on chip in 28-nm cmos. *IEEE J. Solid-State Circuits* **54**, 158–172 (2018).
15. Hirtzlin, T., Bocquet, M., Penkovsky, B., Klein, J.-O., Nowak, E., Vianello, E., Portal, J.-M. & Querlioz, D. Digital biologically plausible implementation of binarized neural networks with differential hafnium oxide resistive memory arrays. *Front. Neurosci.* (2019).
16. Lin, X., Zhao, C. & Pan, W. Towards accurate binary convolutional neural network. In *Advances in Neural Information Processing Systems*, 345–353 (2017).
17. Penkovsky, B., Bocquet, M., Hirtzlin, T., Klein, J.-O., Nowak, E., Vianello, E., Portal, J.-M. & Querlioz, D. In-memory resistive ram implementation of binarized neural networks for medical applications. In *Design, Automation and Test in Europe Conference (DATE)* (2020).
18. Shin, H., Lee, J. K., Kim, J. & Kim, J. Continual learning with deep generative replay. In *Advances in Neural Information Processing Systems*, 2990–2999 (2017).
19. Rebuffi, S.-A., Kolesnikov, A., Sperl, G. & Lampert, C. H. icarl: Incremental classifier and representation learning. In *Proceedings of the IEEE conference on Computer Vision and Pattern Recognition*, 2001–2010 (2017).
20. Li, Z. & Hoiem, D. Learning without forgetting. *IEEE transactions on pattern analysis machine intelligence* **40**, 2935–2947 (2017).
21. Zenke, F., Poole, B. & Ganguli, S. Continual learning through synaptic intelligence. In *Proceedings of the 34th International Conference on Machine Learning-Volume 70*, 3987–3995 (JMLR. org, 2017).

22. Aljundi, R., Babiloni, F., Elhoseiny, M., Rohrbach, M. & Tuytelaars, T. Memory aware synapses: Learning what (not) to forget. In *Proceedings of the European Conference on Computer Vision (ECCV)*, 139–154 (2018).
23. Kingma, D. P. & Ba, J. Adam: A method for stochastic optimization. *arXiv preprint arXiv:1412.6980* (2014).
24. Xiao, H., Rasul, K. & Vollgraf, R. Fashion-mnist: a novel image dataset for benchmarking machine learning algorithms. *arXiv preprint arXiv:1708.07747* (2017).
25. Editorial. Big data needs a hardware revolution. *Nature* **554**, 145, DOI: [10.1038/d41586-018-01683-1](https://doi.org/10.1038/d41586-018-01683-1) (2018).
26. Ambrogio, S., Narayanan, P., Tsai, H., Shelby, R. M., Boybat, I., di Nolfo, C., Sidler, S., Giordano, M., Bodini, M., Farinha, N. C. *et al.* Equivalent-accuracy accelerated neural-network training using analogue memory. *Nature* **558**, 60–67 (2018).
27. Boyn, S., Grollier, J., Lecerf, G., Xu, B., Locatelli, N., Fusil, S., Girod, S., Carrétéro, C., Garcia, K., Xavier, S. *et al.* Learning through ferroelectric domain dynamics in solid-state synapses. *Nat. communications* **8**, 1–7 (2017).
28. Romera, M., Talatchian, P., Tsunegi, S., Araujo, F. A., Cros, V., Bortolotti, P., Trastoy, J., Yakushiji, K., Fukushima, A., Kubota, H., Yuasa, S., Ernoult, M., Vodenicarevic, D., Hirtzlin, T., Locatelli, N., Querlioz, D. & Grollier, J. Vowel recognition with four coupled spin-torque nano-oscillators. *Nature* **563**, 230 (2018).
29. Torrejon, J., Riou, M., Araujo, F. A., Tsunegi, S., Khalsa, G., Querlioz, D., Bortolotti, P., Cros, V., Yakushiji, K., Fukushima, A. *et al.* Neuromorphic computing with nanoscale spintronic oscillators. *Nature* **547**, 428 (2017).
30. Diaconis, P. & Shahshahani, M. The subgroup algorithm for generating uniform random variables. *Probab. engineering informational sciences* **1**, 15–32 (1987).
31. Ioffe, S. & Szegedy, C. Batch normalization: Accelerating deep network training by reducing internal covariate shift. *arXiv preprint arXiv:1502.03167* (2015).



## Supplementary Note 1: Forward and Backward Propagation in Binarized Neural Networks

**Supplementary Algorithm 1** Forward function of the BNN reproduced from<sup>11</sup>.  $W^b = (W_l^b)_{l=1\dots L}$  are the binary weights,  $W^{BN} = \{(\gamma_l, \beta_l) \mid l = 1\dots L\}$  are Batch Normalization parameters.  $L$  is the total number of layers and the subscript  $l$  when specified is the layer index.  $x$  is a batch of input data with dimensions  $(P, N)$  with  $P$  the number of pixels and  $N$  the number of examples in the batch.  $E(\cdot)$  and  $Var(\cdot)$  are batch-wise mean and variance. While they are computed during training with the statistics of the batches, running averages of the mean and variance are stored to be used at test time. This enables the network to infer on a single example at test time.  $\varepsilon$  is a small number to avoid division by zero, it was set to  $10^{-5}$  in all the experiments.

*Input:*  $W^b, W^{BN}, x$ .

*Output:*  $\hat{y}$ , cache.

```

1:  $a_0 \leftarrow x$                                 ▷ Input is not binarized
2: for  $l = 1$  to  $L$  do                            ▷ For loop over the layers
3:    $z_l \leftarrow W_l^b a_l$                         ▷ Matrix multiplication
4:    $a_l \leftarrow \gamma_l \cdot \frac{z_l - E(z_l)}{\sqrt{Var(z_l) + \varepsilon}} + \beta_l$   ▷ Batch Normalization31
5:   if  $l < L$  then                                ▷ If not the last layer
6:      $a_l^b \leftarrow \text{Sign}(a_l)$                     ▷ Activation is binarized
7:   end if
8: end for
9:  $\hat{y} \leftarrow a_L$ 
10: return  $\hat{y}$ , cache

```

**Supplementary Algorithm 2** Backward function of the BNN reproduced from<sup>11</sup>.  $W^b = (W_l^b)_{l=1\dots L}$  are the binary weights,  $\theta^{BN} = \{(\gamma_l, \beta_l) \mid l = 1\dots L\}$  are Batch Normalization parameters.  $\text{BackBatchNorm}(\cdot)$  specifies how to backpropagate through the Batch normalization<sup>31</sup>.  $L$  is the total number of layers and the subscript  $l$  when specified is the layer index.  $1_{|a_l| \leq 1}$  is the derivative of Hardtanh taken as a replacement for back propagating through Sign activation.

*Input:*  $C, \hat{y}, W^b, \theta^{BN}$ , cache.

*Output:*  $(\partial_W C, \partial_\theta C)$ .

```

1:  $g_{a_L} \leftarrow \frac{\partial C}{\partial \hat{y}}$                                 ▷ Cost gradient with respect to output
2: for  $l = L$  to 1 do                                    ▷ For loop backward over the layers
3:   if  $l < L$  then                                        ▷ If not the last layer
4:      $g_{a_l} \leftarrow g_{a_l^b} \cdot 1_{|a_l| \leq 1}$             ▷ Back Prop through Sign
5:   end if
6:    $(g_{z_l}, g_{\gamma_l}, g_{\beta_l}) \leftarrow \text{BackBatchNorm}(g_{a_l}, z_l, \gamma_l, \beta_l)$   ▷ See31
7:    $g_{a_{l-1}^b} \leftarrow W_l^b g_{z_l}$ 
8:    $g_{W_l^b} \leftarrow a_{l-1}^{b \top} g_{z_l}$ 
9: end for
10:  $\partial_W C \leftarrow \{g_{W_l^b} \mid l = 1\dots L\}$ 
11:  $\partial_\theta C \leftarrow \{g_{\gamma_l}, g_{\beta_l} \mid l = 1\dots L\}$ 
12: return  $(\partial_W C, \partial_\theta C)$ 

```

The optimization is performed using Adaptive Moment Estimation (Adam) algorithm<sup>23</sup>. As the sign function is not differentiable in zero and the derivative is zero on  $\mathbb{R}^*$ , during error backpropagation the derivative of hardtanh function is used as a replacement for the derivative of the Sign function. The activation function is the sign function

except for the output layer. The input neurons are not binarized. We use batch normalization<sup>31</sup> at all layers as detailed in Alg. 1. The following derivation for layer  $l$ ,

$$\gamma_l \cdot \frac{z - E(z)}{\sqrt{\text{Var}(z) + \epsilon}} + \beta_l = \frac{\gamma_l}{\sqrt{\text{Var}(z) + \epsilon}} \left( z - \left[ E(z) - \frac{\beta_l \sqrt{\text{Var}(z) + \epsilon}}{\gamma_l} \right] \right)$$

$$a = \text{Sign}(\gamma_l) \text{Sign} \left( z - \left[ E(z) - \frac{\beta_l \sqrt{\text{Var}(z) + \epsilon}}{\gamma_l} \right] \right)$$

shows that because the Sign function is invariant by any multiplicative constant in the input, the only task dependent parameters we need to store for an inference hardware chip is the term between square brackets, along with the sign of  $\gamma_l$ . The amount of task dependent parameters scales as the number of neurons and is order of magnitudes smaller than the number of synapses.

Adam optimizer updates the hidden weight with loss gradients computed using binary weights only. We use a small weight decay of  $10^{-7}$  in the Adam optimizer to make zero floating values more stable. However, consolidated weights are not subject to weight decay, as we implement weight decay as a modification of the loss gradient, which is gradually suppressed by  $f_{\text{meta}}$ .

## Supplementary Note 2: Training parameters

Network	pMNISTs		
	Binarized meta	Binarized EWC	Full precision
Layers	784-4096-4096-10	784-4096-4096-10	784-4096-4096-10
Learning rate	0.005	0.005	0.005
Minibatch size	100	100	100
Epochs/task	40	40	40
$m$	1.5	0.0	1.5
$\lambda_{\text{EWC}}$	0.0	5,000	0.0
Weight decay	1e-7	1e-7	1e-7
Initialization	Uniform width = 0.1	Uniform width = 0.1	Uniform width = 0.1

**Table 2.** Hyperparameters for the permuted MNISTs experiment.

FMNIST - MNIST	
Network	Binarized meta
Layers	784-4096-4096-10
Learning rate	0.005
Minibatch size	100
Epochs/task	50
$m$	1.5
Weight decay	1e-8
Initialization	Uniform width = 0.1

**Table 3.** Hyperparameters for the permuted FMNIST-MNIST experiment.

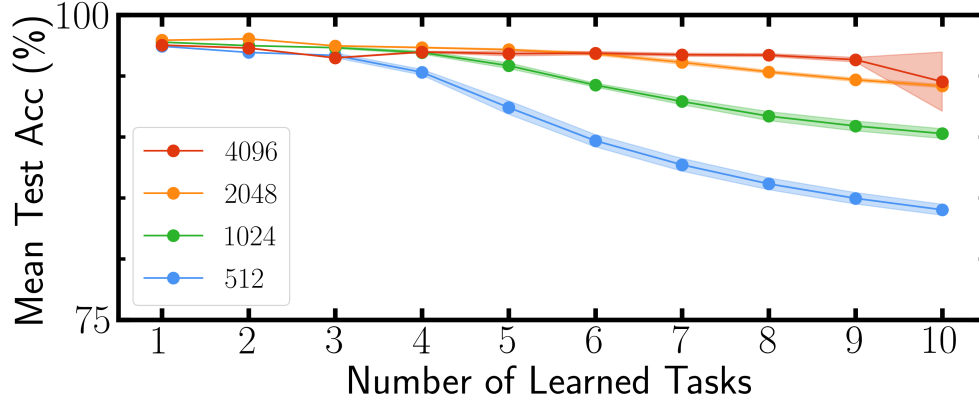
The batch normalization layers parameters were not learned for the Fashion MNIST experiment whereas they were learned for the CIFAR-10 experiment.

	Stream FMNIST	Stream CIFAR-10
Network	Binarized meta	Binarized meta
Layers	784-1024-1024-10	VGG-7
Sub Parts	60	20
Learning rate	0.005	0.0001
Minibatch size	100	64
Epochs/subset	20	200
$m$	2.5	13.0
Weight decay	1e-7	0.0
Initialization	Uniform width = 0.1	Gauss width = 0.007

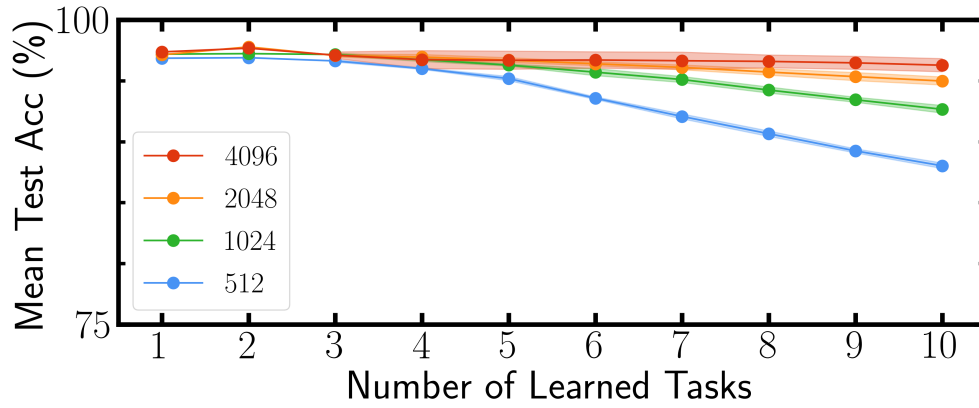
**Table 4.** Hyperparameters for the stream learning experiment.

The batch normalization parameters are set to  $\beta = 0$ ,  $\gamma = 1$  for the Fashion MNIST experiment. The performance of the BNN with learned batch normalization parameters was inferior, as batch normalization parameters appear to overfit to the subsets of data. In the CIFAR-10 experiment the performance was higher with learned batch normalization parameters. The architecture of VGG-7 network consists of 6 convolutional layers of  $3 \times 3$  sized kernels with kernel number per layer following the sequence 128-128-256-256-512-512. The classifier consists of two hidden layers of 2048-1024 hidden units. Dropout was used in the classifier with value 0.5.

(a) Metaplasticity



(b) EWC



**Supplementary Figure 6. Influence of the network size on the number of tasks learned.** Mean test accuracy over tasks learned so far for up to ten tasks. Each task is a permuted version of MNIST learned for 40 epochs. The binarized neural network architecture consists of two hidden layers of a variable number of hidden units ranging from 512 to 4096. (a) uses metaplasticity with parameter  $m = 1.35$  and (b) uses elastic weight consolidation with  $\lambda_{\text{EWC}} = 5,000$ . The decrease in mean test accuracy comes from the impossibility to learn new tasks because too many weights are consolidated.

### Supplementary Note 3: Mathematical proofs

**Definition 1** (Quadratic Binary Task). *Consider the loss function:*

$$\mathcal{L}(W) = \frac{1}{2}(W - W^*)^T \cdot H \cdot (W - W^*) \quad (7)$$

with a symmetric definite positive matrix  $H \in \mathbb{R}^{d \times d}$ . Gradients are given by  $g(W) = H \cdot (W - W^*)$ . We assume the following optimization scheme:

$$W_{t+1}^h = W_t^h - \eta H \cdot (\text{sign}(W_t^h) - W^*), \quad (8)$$

where  $\text{sign}$  returns the sign of a vector component-wise.

**Lemma 1** (Condition for hidden Weight confinement ). *Let  $W^h$  optimize a quadratic binary task according to the dynamics  $W_{t+1}^h = W_t^h - \eta H(\text{sign}(W_t^h) - W^*)$ . Let  $\mathcal{B}_\infty$  be the unit ball for the infinite norm and  $\overline{\mathcal{B}_\infty}$  its closure. Then:*

$$W^* \in \mathcal{B}_\infty \Rightarrow \exists C > 0, \forall t \in \mathbb{N}, \|W_t^h\|_\infty < C \quad (9)$$

$$W^* \notin \overline{\mathcal{B}_\infty} \Rightarrow \lim_{t \rightarrow \infty} \|W_t^h\|_\infty = \infty \quad (10)$$

*Proof of Lemma 1.* We first prove Eq. (10). Let us assume that  $W^* \notin \overline{\mathcal{B}_\infty}$  so that there exists at least one component  $i \in \llbracket 1, d \rrbracket$  such that  $|W_i^*| > 1$ . Since  $H$  is symmetric definite positive, it is invertible. Taking the euclidian scalar product between  $H^{-1}e_i$  and the update  $(W_{t+1}^h - W_t^h)$  yields:

$$\begin{aligned} \langle e_i, W_{t+1}^h - W_t^h \rangle_{H^{-1}} &= (H^{-1}e_i)^T \cdot (W_{t+1}^h - W_t^h) \\ &= -\eta (H^{-1}e_i)^T \cdot H(\text{sign}(W_t^h) - W^*) \\ &= -\eta e_i^T \cdot (H^{-1})^T H(\text{sign}(W_t^h) - W^*) \\ &= -\eta e_i^T \cdot H^{-1} H(\text{sign}(W_t^h) - W^*) \\ &= -\eta e_i^T \cdot (\text{sign}(W_t^h) - W^*) \\ &= -\eta (\text{sign}(W_{i,t}^h) - W_i^*), \end{aligned}$$

where we have used at the fourth equality that  $H^{-1}$  is also symmetric. Since  $|W_i^*| > 1$ , the sign of  $\text{sign}(W_{i,t}^h) - W_i^*$  is constant (and  $\neq 0$ ), so the component of  $W$  along  $H^{-1}e_i$  is expected to diverge. More precisely, let us assume  $W_i^* > 1$  so that  $\text{sign}(W_{i,t}^h) - W_i^* < 1 - W_i^*$  and:

$$\langle e_i, W_{t+1}^h - W_t^h \rangle_{H^{-1}} \geq -\eta(1 - W_i^*). \quad (11)$$

Summing Eq. (11) from time step 0 to  $t$  yields:

$$\langle e_i, W_t^h \rangle_{H^{-1}} \geq -\eta(1 - W_i^*)t + \langle e_i, W_0^h \rangle_{H^{-1}}, \quad (12)$$

showing that  $\lim_{t \rightarrow +\infty} \langle e_i, W_t^h \rangle_{H^{-1}} = +\infty$ . Consequently there exists  $j \in \llbracket 1, d \rrbracket$  such that  $\lim_{t \rightarrow +\infty} \langle e_j, W_t^h \rangle = +\infty$  and therefore  $\lim_{t \rightarrow \infty} \|W_t^h\|_\infty = +\infty$ . Similarly if  $W_i^* < -1$ , we show that:

$$\langle e_i, W_t^h \rangle_{H^{-1}} \leq \eta(1 + W_i^*)t + \langle e_i, W_0^h \rangle_{H^{-1}}, \quad (13)$$

giving the same conclusion as above.

We now prove Eq. (9). Let us assume that  $W^* \in \mathcal{B}_\infty$ , i.e.  $\forall i \in \llbracket 1, d \rrbracket$ ,  $|W_i^*| < 1$ . We have:

$$\begin{aligned}
\|W_{t+1}^h\|_{H^{-1}}^2 &= \langle W_{t+1}^h, W_{t+1}^h \rangle_{H^{-1}} \\
&= \langle W_t^h + \Delta W_t^h, W_t^h + \Delta W_t^h \rangle_{H^{-1}} \\
&= \|W_t^h\|_{H^{-1}}^2 + 2\langle \Delta W_t^h, W_t^h \rangle_{H^{-1}} + \langle \Delta W_t^h, \Delta W_t^h \rangle_{H^{-1}} \\
&= \|W_t^h\|_{H^{-1}}^2 + 2\langle H^{-1} \Delta W_t^h, W_t^h \rangle + \|\Delta W_t^h\|_{H^{-1}}^2 \\
&= \|W_t^h\|_{H^{-1}}^2 - 2\eta(\text{sign}(W_t^h) - W^*)^T W_t^h + \|\Delta W_t^h\|_{H^{-1}}^2 \\
&= \|W_t^h\|_{H^{-1}}^2 - 2\eta(\text{sign}(W_t^h) - W^*)^T W_t^h + \|\Delta W_t^h\|_{H^{-1}}^2,
\end{aligned}$$

so that :

$$\begin{aligned}
\|W_{t+1}^h\|_{H^{-1}}^2 - \|W_t^h\|_{H^{-1}}^2 &\leq 0 \\
\Leftrightarrow 2(\text{sign}(W_t^h) - W^*)^T \cdot W_t^h &\geq \|\Delta W_t^h\|_{H^{-1}}^2.
\end{aligned} \tag{14}$$

We want to show that if  $W_t^h$  is large enough in norm  $\|\cdot\|_{H^{-1}}$ , Eq. (14) will be met. First note that, because the dimension is finite there exist two constants  $\alpha > 0$  and  $\beta > 0$  such that  $\forall x \in \mathbb{R}^d$ ,

$$\alpha \|x\|_{H^{-1}} < \|x\|_\infty < \beta \|x\|_{H^{-1}}$$

and also that:

$$\|\Delta W_t^h\|_{H^{-1}}^2 = \eta^2 \|\text{sign}(W_t^h) - W^*\|_H^2.$$

Then, by triangular inequality:

$$\eta \|\text{sign}(W_t^h) - W^*\|_H \leq \eta (\|\text{sign}(W_t^h)\|_H + \|W^*\|_H).$$

Denoting  $(e_\alpha)_\alpha$  and  $(\lambda_\alpha)_\alpha$  the eigenbasis of  $H$  and their associated eigenvalues, we have by Cauchy Schwarz inequality:

$$\begin{aligned}
\|\text{sign}(W_t^h)\|_H^2 &= \langle H \cdot \text{sign}(W_t^h), \text{sign}(W_t^h) \rangle \\
&= \sum_{\alpha=1}^d \lambda_\alpha |\langle \text{sign}(W_t^h), e_\alpha \rangle|^2 \\
&\leq \sum_{\alpha=1}^d \lambda_\alpha \underbrace{\|\text{sign}(W_t^h)\|_2^2}_{=d} \cdot \underbrace{\|e_\alpha\|_2^2}_{=1} \\
&\leq d^2 \lambda_{\alpha, \max},
\end{aligned}$$

so that:

$$\|\Delta W_t^h\|_{H^{-1}} \leq \eta (d \sqrt{\lambda_{\alpha, \max}} + \|W^*\|_H). \tag{15}$$

Thus the right hand side of Eq. 14 is bounded. Also note that:



$$\begin{aligned}
2(\text{sign}(W_t^h) - W^*)^T \cdot W_t^h &= 2 \sum_{i=1}^d (1 - \text{sign}(W_{i,t}^h) W_i^*) |W_{i,t}^h| \\
&\geq 2 \sum_{i=1}^d (1 - |W_i^*|) |W_{i,t}^h| \\
&\geq 2(1 - \|W^*\|_\infty) \sum_{i=1}^d |W_{i,t}^h| \\
&\geq 2(1 - \|W^*\|_\infty) \cdot \|W_t^h\|_\infty,
\end{aligned}$$

So far we have shown that the left hand side of Eq. 14 is lower bounded by a constant ( $\neq 0$ ) times the infinite norm of  $W_t^h$ , while the right hand side is bounded. Therefore to ensure Eq. (14) it suffices that:

$$\begin{aligned}
2(1 - \|W^*\|_\infty) \cdot \|W_t^h\|_\infty &\geq \eta(d\sqrt{\lambda_{\alpha, \max}} + \|W^*\|_H) \\
\Leftrightarrow \|W_t^h\|_\infty &\geq \frac{\eta(d\sqrt{\lambda_{\alpha, \max}} + \|W^*\|_H)}{2(1 - \|W^*\|_\infty)}.
\end{aligned}$$

And thus to ensure Eq. (14) it suffices that:

$$\|W_t^h\|_{H^{-1}} \geq \frac{\eta(d\sqrt{\lambda_{\alpha, \max}} + \|W^*\|_H)}{2\alpha(1 - \|W^*\|_\infty)}.$$

Denoting  $M = \frac{\eta(d\sqrt{\lambda_{\alpha, \max}} + \|W^*\|_H)}{2\alpha(1 - \|W^*\|_\infty)}$ , we can conclude that  $\|W_t^h\|_{H^{-1}} \geq M \Rightarrow \|W_{t+1}^h\|_{H^{-1}}^2 < \|W_t^h\|_{H^{-1}}^2$ . And because the update  $\Delta W_t^h$  is bounded in norm  $\|\cdot\|_{H^{-1}}$ , an absolute upper bound of  $W_t^h$  is :

$$C = \beta \max(\|W_0^h\|_{H^{-1}}, M + \eta(d\sqrt{\lambda_{\alpha, \max}} + \|W^*\|_H)).$$

Thus we have proven that  $W^* \in \mathcal{B}_\infty \Rightarrow \exists C > 0, \forall t \in \mathbb{N}, \|W_t^h\|_\infty < C$

□

**Lemma 2** (hidden Weight Trajectory). *Let  $W^h$  optimize a quadratic binary task according to the dynamics  $W_{t+1}^h = W_t^h - \eta H(\text{sign}(W_t^h) - W^*)$  and assume  $H = \text{diag}(\lambda_1, \dots, \lambda_d)$ . Then:*

$$|W_i^*| > 1 \implies W_{i,t}^h \sim_{t \rightarrow +\infty} \underbrace{\text{sign}(W_i^*) \eta \lambda_i (|W_i^*| - 1)}_{= \widehat{W}_i^h} t \quad (16)$$

*Proof of Lemma 2.* If  $H = \text{diag}(\lambda_1, \dots, \lambda_d)$ , the dynamics of  $W_t^h$  defined in Eq. (8) simply rewrites component-wise:

$$\forall i \in \llbracket 1, d \rrbracket, \Delta W_{i,t}^h = W_{i,t+1}^h - W_{i,t}^h = -\eta \lambda_i (\text{sign}(W_{i,t}^h) - W_i^*). \quad (17)$$

By Lemma 1, components  $W_i$  such that  $|W_i^*| < 1$  are bounded.

For components  $i$  where  $|W_i^*| > 1$ ,  $\Delta W_{i,t}^h$  has the sign of  $W_i^*$  since Eq. (17) rewrites:

$$\Delta W_{i,t}^h = \text{sign}(W_i^*) \underbrace{\eta \lambda_i (|W_i^*| - \text{sign}(W_i^* W_{i,t}^h))}_{>0}, \quad (18)$$

so that  $W_{i,t}^h$  necessarily ends up having the same sign as  $W_i^*$ , hence there exists  $t_{0,i} \in \mathbb{N}$  such that :

$$\forall t > t_{0,i}, \quad \Delta W_{i,t}^h = \text{sign}(W_i^*) \eta \lambda_i (|W_i^*| - 1). \quad (19)$$

By definition of  $t_{0,i}$ ,  $W_{i,t}^h$  and  $W_i^*$  have opposite sign before  $t_{0,i}$  so that:

$$\forall t \leq t_{0,i}, \quad \Delta W_{i,t}^h = \text{sign}(W_i^*) \eta \lambda_i (1 + |W_i^*|). \quad (20)$$

Therefore, summing Eq. (17) between 0 and  $t$  yields :

$$\begin{aligned} W_{i,t}^h &= W_{i,0}^h + \sum_{u=0}^{t_{0,i}} \text{sign}(W_i^*) \eta \lambda_i (|W_i^*| + 1) \\ &\quad + \sum_{u=t_{0,i}+1}^t \text{sign}(W_i^*) \eta \lambda_i (|W_i^*| - 1) \\ &= W_{i,0}^h + \text{sign}(W_i^*) \eta \lambda_i (|W_i^*| + 1) t_{0,i} \\ &\quad + \text{sign}(W_i^*) \eta \lambda_i (|W_i^*| - 1) (t - t_{0,i}) \\ &\sim_{t \rightarrow +\infty} \underbrace{\text{sign}(W_i^*) \eta \lambda_i (|W_i^*| - 1) t}_{=\widetilde{W}_i^h} \end{aligned} \quad (21)$$

□

**Theorem 2** (Importance of hidden Weights in a quadratic binary task). *Let  $W$  optimize a quadratic binary task according to the dynamics  $W_{t+1}^h = W_t^h - \eta H(\text{sign}(W_t^h) - W^*)$  and assume  $H = \text{diag}(\lambda_1, \dots, \lambda_d)$ . Then, for any component  $i$  such that  $|W_i^*| > 1$ , the variation of loss resulting from flipping  $\text{sign}(W_{i,t}^h) \rightarrow -\text{sign}(W_{i,t}^h)$  is:*

$$\Delta_i \mathcal{L}(W_t^h) = 2\lambda_i |W_i^*| = 2 \left( \lambda_i + \frac{|\widetilde{W}_i^h|}{\eta} \right) + \mathcal{O}\left(\frac{1}{t}\right) \quad (22)$$

Proof of Theorem. 2

*Proof.* Using Eq. (7), the loss reads:

$$\begin{aligned} \mathcal{L}(W_t^h) &= \frac{1}{2} (\text{sign}(W_t^h) - W^*)^T H (\text{sign}(W_t^h) - W^*) \\ &= \frac{1}{2} \sum_{i=1}^n \lambda_i (\text{sign}(W_{i,t}^h) - W_i^*)^2 \\ &= \frac{1}{2} \sum_{i, |W_i^*| \leq 1} \lambda_i (\text{sign}(W_{i,t}^h) - W_i^*)^2 \\ &\quad + \frac{1}{2} \sum_{i, |W_i^*| > 1} \lambda_i (\text{sign}(W_{i,t}^h) - W_i^*)^2. \end{aligned}$$

Using Lemma 2, for all components  $i$  such that  $|W_i^*| > 1$ , there exists  $t_{0,i}$  such that for all  $t > t_{0,i}$ ,  $\text{sign}(W_{i,t}^h) = \text{sign}(W_i^*)$  and therefore  $\frac{1}{2}\lambda_i(\text{sign}(W_{i,t}^h) - W_i^*)^2 = \frac{1}{2}\lambda_i(1 - |W_i^*|)^2$ . Defining  $T = \max_{i||W_i^*|>1}(t_{0,i})$ , the loss rewrites for  $t > T$  :

$$\begin{aligned}\mathcal{L}(W_t^h) &= \frac{1}{2} \sum_{i, |W_i^*| \leq 1} \lambda_i (\text{sign}(W_{i,t}^h) - W_i^*)^2 \\ &\quad + \frac{1}{2} \sum_{i, |W_i^*| > 1} \lambda_i (|W_i^*| - 1)^2\end{aligned}$$

Then, the increase in energy if a binary component in the  $|W_i^*| > 1$  sum is switched is :

$$\Delta_i \mathcal{L}(W_t^h) = \frac{\lambda_i}{2} ((|W_i^*| + 1)^2 - (|W_i^*| - 1)^2) = 2\lambda_i |W_i^*| \quad (23)$$

Using the explicit form of  $W_{i,t}^h$  in Eq. (21) along with Eq. (23), we get:

$$\begin{aligned}W_{i,t}^h &= W_{i,0}^h + \text{sign}(W_i^*) \eta \lambda_i (|W_i^*| + 1) t_{0,i} \\ &\quad + \text{sign}(W_i^*) \eta \lambda_i (|W_i^*| - 1) (t - t_{0,i}) \\ &= W_{i,0}^h + \text{sign}(W_i^*) \eta \lambda_i \left( \frac{\Delta_i \mathcal{L}}{2\lambda_i} + 1 \right) t_{0,i} \\ &\quad + \text{sign}(W_i^*) \eta \lambda_i \left( \frac{\Delta_i \mathcal{L}}{2\lambda_i} - 1 \right) (t - t_{0,i}) \\ &= W_{i,0}^h + \text{sign}(W_i^*) \eta \frac{\Delta_i \mathcal{L}}{2} t + \text{sign}(W_i^*) \eta \lambda_i (2t_{0,i} - t) \\ &= \text{sign}(W_i^*) \eta \left( \frac{\Delta_i \mathcal{L}}{2} - \lambda_i \right) t + W_{i,0}^h + \text{sign}(W_i^*) \eta \lambda_i 2t_{0,i}.\end{aligned}$$

Since  $W_{i,t}^h$  has the same sign as  $W_i^*$  for  $t$  being large enough, multiplying both sides for the last equation and dividing by  $t$  yields:

$$\Delta_i \mathcal{L}(W_t^h) = 2 \left( \lambda_i + \frac{|\widetilde{W}_i^h|}{\eta} \right) \underbrace{-2 \frac{|W_{i,0}^h| + \eta \lambda_i 2t_{0,i}}{\eta t}}_{=\mathcal{O}(\frac{1}{t})} \quad (24)$$

□